Distinct roles of adipose triglyceride lipase and hormone-sensitive lipase in the catabolism of triacylglycerol estolides

Kristyna Brejchova[a,1], Franz Peter Walter Radner[b,1], Laurence Balas[c], Veronika Paluchova[a], Tomas Cajka[a], Hana Chodounska[d], Eva Kudova[d], Margarita Schratter[b], Renate Schreiber[b], Thierry Durand[c], Rudolf Zechner[b,e,2], and Ondrej Kuda[a,2]

[a]Institute of Physiology, Czech Academy of Sciences, 142 20 Prague 4, Czech Republic; [b]Institute of Molecular Biosciences, University of Graz, 8010 Graz, Austria; [c]Institut des Biomolécules Max Mousseron, UMR 5247, CNRS, École Nationale Supérieure de Chimie de Montpellier, Faculté de Pharmacie, Université de Montpellier, 34093 Montpellier, France; [d]Institute of Organic Chemistry and Biochemistry, Czech Academy of Sciences, 166 10 Prague 6, Czech Republic; and [e]BioTechMed-Graz, 8010 Graz, Austria

Contributed by Rudolf Zechner, November 13, 2020 (sent for review October 7, 2020; reviewed by Robert V. Farese Jr. and Stephen G. Young)

Branched esters of palmitic acid and hydroxy stearic acid are antiinflammatory and antidiabetic lipokines that belong to a family of fatty acid (FA) esters of hydroxy fatty acids (HFAs) called FAHFAs. FAHFAs themselves belong to oligomeric FA esters, known as estolides. Glycerol-bound FAHFAs in triacylglycerols (TAGs), named TAG estolides, serve as metabolite reservoir of FAHFAs mobilized by lipases upon demand. Here, we characterized the involvement of two major metabolic lipases, adipose triglyceride lipase (ATGL) and hormone-sensitive lipase (HSL), in TAG estolide and FAHFA degradation. We synthesized a library of 20 TAG estolide isomers with FAHFAs varying in branching position, chain length, saturation grade, and position on the glycerol backbone and developed an in silico mass spectra library of all predicted catabolic intermediates. We found that ATGL alone or coactivated by comparative gene identification-58 efficiently liberated FAHFAs from TAG estolides with a preference for more compact substrates where the estolide branching point is located near the glycerol ester bond. ATGL was further involved in transesterification and remodeling reactions leading to the formation of TAG estolides with alternative acyl compositions. HSL represented a much more potent estolide bond hydrolase for both TAG estolides and free FAHFAs. FAHFA and TAG estolide accumulation in white adipose tissue of mice lacking HSL argued for a functional role of HSL in estolide catabolism in vivo. Our data show that ATGL and HSL participate in the metabolism of estolides and TAG estolides in distinct manners and are likely to affect the lipokine function of FAHFAs.

ATGL | HSL | FAHFA | lipokine

Branched esters of palmitic acid and hydroxy stearic acid (PAHSAs) are antiinflammatory and antidiabetic lipokines (1–3). PAHSA serum and adipose tissue levels correlate with insulin sensitivity and are decreased in insulin-resistant humans (2, 4). PAHSAs increase glucose-stimulated insulin secretion by enhancing the production of the gut-derived incretin glucagon-like peptide-1 (5, 6). The antiinflammatory effects of PAHSA isomers (2, 7, 8) are mediated via free fatty acid receptor 4 (FFAR4, GPR120) and modulate both innate and adaptive immune responses in a mouse colitis model (1) and type-1 diabetes (6). Therefore, PAHSAs have beneficial effects on both metabolism and the immune system (9).

PAHSAs belong to the family of fatty acid (FA) esters of hydroxy FAs (HFAs) called FAHFAs, which are part of a much larger family of mono- or oligomeric FAHFA esters named estolides. Since FAHFAs contain only a single ester bond of one FA with one HFA (the estolide bond), they represent monoestolides (10). The position of the branching carbon atom defines the regioisomer (e.g., 5-PAHSA or 9-PAHSA). PAHSAs and other less-well-studied FAHFAs such as the oleic acid esters of hydroxy palmitic acid (OAHPAs) or the docosahexaenoic acid ester of 13-hydroxy linoleic acid (13-DHAHLA) derive from either dietary sources or de novo synthesis in adipose tissue and other organs (2, 11, 12). Nonesterified, free FAHFAs (free monoestolides) can be esterified to glycerol to form FAHFA acylglycerols, which in combination with other FAs result in the formation of triacylglycerol (TAG) estolides, diacylglycerol (DAG) estolides, or monoacylglycerol (MAG) estolides. TAG estolides represent a major storage form of bioactive free FAHFAs and are present in plant oils (e.g., castor oil) (13, 14) and adipose tissue of mice (3, 15) and humans (16).

Both the synthetic and catabolic pathways of FAHFAs and TAG estolides are insufficiently understood. The hydrolytic catabolism of FAHFAs and TAG estolides results in the generation of highly bioactive and physiologically relevant FAHFAs, HFAs, FAs, and DAGs. Given the structural and metabolic similarity between TAGs and TAG estolides, it seemed reasonable to suspect that canonical TAG lipases will be involved in FAHFA and TAG estolide degradation. Generally, the catabolism of TAGs in cells occurs in the cytosol (neutral lipolysis) or in lysosomes (acidic lipolysis). Neutral lipolysis represents the predominant pathway for the hydrolysis of lipid droplet-associated TAGs in adipocytes involving three major enzymes, adipose

Significance

Fat mass is controlled by the balance of triacylglycerol (TAG) degradation and synthesis. Adipose triglyceride lipase (ATGL) and hormone-sensitive lipase (HSL) are key players in TAG catabolism providing fatty acids (FAs) as energy substrates and metabolic intermediates. Here, we show that ATGL and HSL metabolize TAGs containing antidiabetic lipid mediators (FA esters of hydroxy FAs), distinctly controlling the release of bioactive lipids. Our paper connects lipolysis-mediated TAG metabolism with the regulation of antidiabetic signaling lipids.

Author contributions: R.Z. and O.K. designed research; K.B., F.P.W.R., L.B., V.P., T.C., H.C., E.K., M.S., R.S., T.D., and O.K. performed research; L.B., H.C., E.K., R.S., T.D., R.Z., and O.K. contributed new reagents/analytic tools; K.B., F.P.W.R., V.P., T.C., M.S., R.S., R.Z., and O.K. analyzed data; and K.B., F.P.W.R., L.B., T.C., E.K., R.S., T.D., R.Z., and O.K. wrote the paper.

Reviewers: R.V.F., Harvard Medical School; and S.G.Y., University of California, Los Angeles.

The authors declare no competing interest.

[1]K.B. and F.P.W.R. contributed equally to this work.

[2]To whom correspondence may be addressed. Email: rudolf.zechner@uni-graz.at or ondrej.kuda@fgu.cas.cz.

This article contains supporting information online at https://www.pnas.org/lookup/suppl/doi:10.1073/pnas.2020999118/-/DCSupplemental.

Published December 28, 2020.

triglyceride lipase (ATGL), hormone-sensitive lipase (HSL), and monoglyceride lipase (MGL). ATGL catalyzes the initial step of TAG hydrolysis, generating DAG and one FA (3, 17, 18). The enzyme belongs to the patatin-like phospholipase domain-containing (PNPLA) family of proteins comprising a number of lipid hydrolases (3, 15). ATGL is the most potent TAG hydrolase within this family but also exhibits some phospholipase, retinylesterase, and transacylase activities of undefined physiological relevance (17, 19, 20). For full TAG hydrolase activity, ATGL requires a coactivator named comparative gene identification-58 (CGI-58; also called α/β-hydrolase domain containing 5, ABHD5) (21–23). CGI-58 features α/β-hydrolase folds and also exerts some

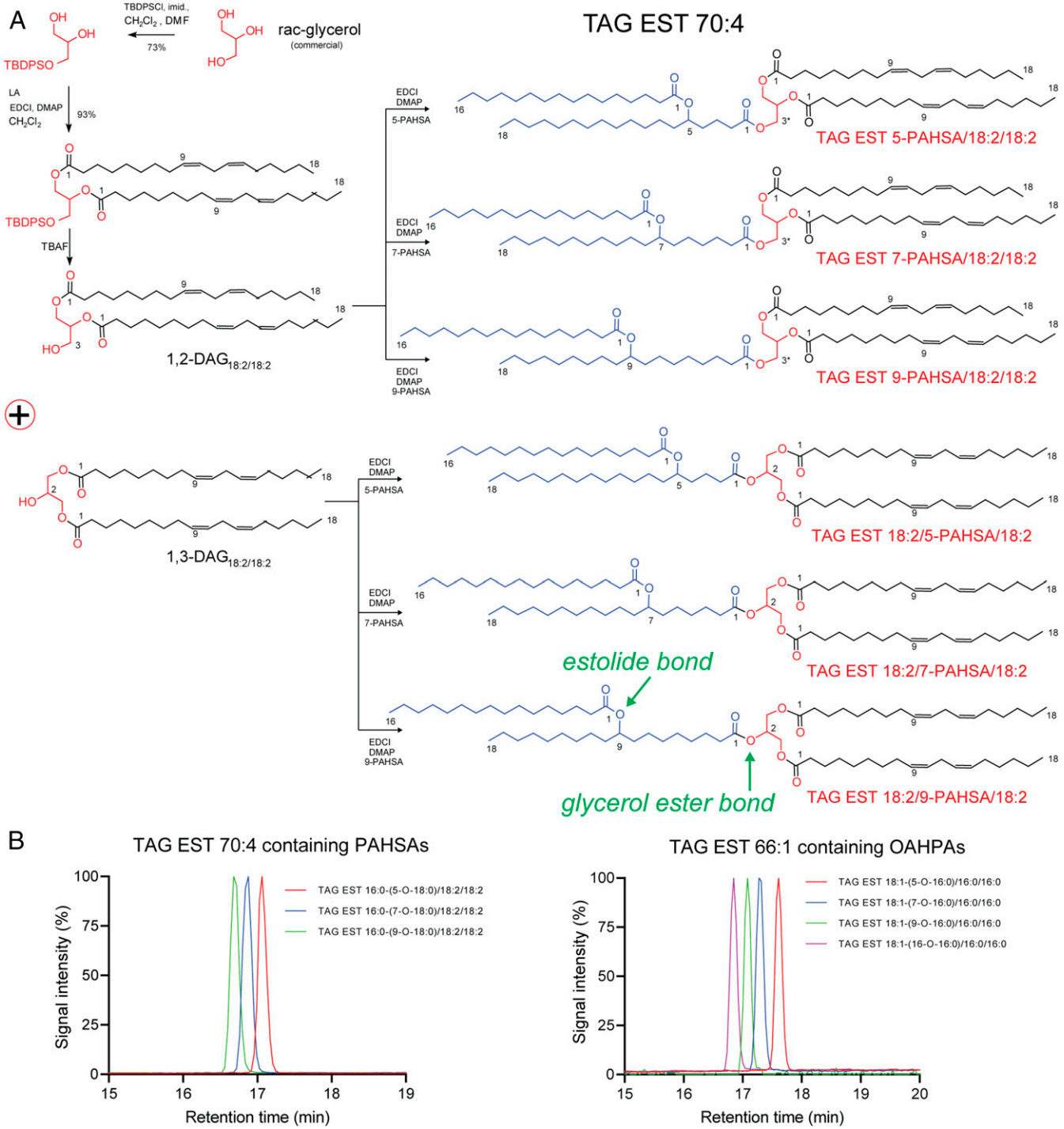

Fig. 1. Synthesis of TAG estolide 70:4 isomers. (*A*) Scheme of the organic synthesis of TAG estolide (TAG EST) 70:4 isomers. 1,2- and 1,3-dilinoleoyl glycerol (1,2/1,3-$DAG_{18:2/18:2}$) were esterified with palmitic acid ester of hydroxy stearic acid with branching positions at carbon atom 5, 7, or 9 (5-, 7-, or 9-PAHSA). Both *sn*-1 and *sn*-3 products were synthesized, as the starting glycerol (red structure) was a racemic mixture. The internal ester linkage within the PAHSA (blue structure) is the estolide bond (branching position). (*B*) Illustrative chromatograms of the TAG EST 70:4 and 66:1 isomers. The FAHFA (PAHSA or oleic acid ester of hydroxy palmitic acid [OAHPA]) is bound at the *sn*-1/3 position of the glycerol.

acyltransferase and protease activities (23–25). Yet, the physiological role of these activities remains elusive. ATGL exhibits unique regioselectivity for TAG substrates and preferentially hydrolyzes the *sn*-2 position of the glycerol chain of TAGs (26). Upon stimulation of ATGL by CGI-58 this regioselectivity broadens to the *sn*-1 but not the *sn*-3 position (26).

HSL is rate-limiting for the second step of TAG lipolysis converting DAG to one FA and MAG (27). The enzyme preferentially catalyzes DAGs at the *sn*-3 position and cholesteryl esters (28, 29) but also cleaves TAGs (*sn*-1 and *sn*-3 position), retinylesters (30), or medium- and short-chain carboxylic acid glycerol esters (29). The enzyme is structurally unrelated to ATGL and does not require enzyme coactivators. Hormonal stimulation of neutral lipolysis by β-adrenoreceptor agonists such as catecholamines activates both ATGL and HSL by promoting the molecular interaction of ATGL with CGI-58 on the surface of TAG-containing lipid droplets (21, 31) and the translocation of HSL from the cytoplasm to lipid droplets. These processes involve the protein kinase A-dependent phosphorylation of perilipin-1, CGI-58, and HSL (31–33).

Previous studies by Tan et al. (15) and our laboratory (3) demonstrated that ATGL and HSL are both able to hydrolyze FAHFA–glycerol ester bonds of TAG estolides. However, enzyme preferences for this reaction, the substrate requirements, or the contribution of these enzymes to hydrolyze the FA–HFA ester bond (estolide bond) in TAG estolides as well as in free FAHFAs remained unaddressed. Using a newly generated library of TAG estolides, we now show that ATGL and HSL play distinct roles in the formation of TAG estolides by transesterification reactions and the degradation of (TAG) estolides by hydrolysis reactions.

Results

Synthesis and Structural Analysis of a TAG Estolide Library. For the comprehensive analysis of the substrate requirements for TAG estolide hydrolysis by ATGL and HSL, we prepared a library of 20 TAG estolides with various FAHFAs esterified to the *sn*-1/3 or the *sn*-2 position of the glycerol backbone (*SI Appendix*, Fig. S1). We used the previously published synthetic approach (3) to link FAHFAs with various branching positions (5-, 7-, 9-, 10-, and 16-), chain length (C_{16} and C_{18}), and degree of saturation (0 to 2) (34) to dipalmitoylglycerol or dilinoleoylglycerol. As an example, Fig. 1*A* displays the synthesis of the TAG estolide 70:4 subgroup, where 5-, 7-, and 9-PAHSA were esterified to the outer (*sn*-1 or *sn*-3) and inner (*sn*-2) positions of dilinoleoylglycerol, respectively. Since the synthesis was performed with racemic DAGs, the resulting TAG estolides include epimers of the *sn*-2 and the *sn*-1/3 series. Synthesized TAG estolides were analyzed by liquid chromatography tandem mass spectrometry (LC-MS/MS) and NMR. LC-MS/MS analysis involved the initial separation of TAG estolides by reversed-phase LC according to the number of carbon atoms, the number of double bonds, and the position of the branching carbon atom of FAHFAs (exemplified in Fig. 1*B* for the TAG estolide isomers 70:4 and 66:1) and subsequent MS/MS analysis by Q Exactive Plus. Based on these experimental data, we prepared an in silico LC-MS/MS library for MS-DIAL of all theoretical TAG estolides as well as single, double, and triple monoestolides of MAGs, DAGs, and TAGs, respectively. TAG estolides with multiple branching (diestolides and triestolides) were not considered, as such structures have only been detected in plants but not in animals or humans (13, 14).

Glycerol Ester Bond Hydrolysis: ATGL Is the Predominant Hydrolase to Release FAHFAs from TAG Estolides. To explore the substrate specificity of ATGL and HSL for TAG estolides, we overexpressed the respective complementary DNAs (cDNAs) as well as the *LacZ* gene coding for β-galactosidase (β-Gal) as negative control in HEK293T cells and used cell lysates as enzyme sources. Protein expression in lysates was verified by Western blotting analysis (*SI Appendix*, Fig. S2*A*). LC-MS/MS analysis confirmed that ATGL and HSL were enzymatically active (*SI Appendix*, Fig. S2 *B* and *C*). Using standard lipase substrates, ATGL preferentially hydrolyzed triolein, while HSL preferentially hydrolyzed diolein, conforming with the established substrate preference of the enzymes (27). To determine TAG estolide hydrolysis, ATGL- or HSL-overexpressing cell lysates were incubated with phosphatidylcholine/phosphatidylinositol–emulsified TAG estolide substrates and the reaction products were analyzed by LC-MS/MS. The substrate preference of ATGL was assessed in the presence or absence of purified recombinant CGI-58 (21). In the first set of experiments, saturated TAG estolides 66:0 [16:0-(z-O-18:0)/16:0/16:0] with branching positions at z = 5, 7, or 9 were used as substrate. As shown in Fig. 2*A*, ATGL most efficiently catalyzed the release of PAHSAs from the glycerol backbone in the presence of CGI-58 followed by ATGL without coactivator. HSL had only a minor PAHSA-releasing activity compared to ATGL. Interestingly, the PAHSA release via ATGL+ CGI-58 or ATGL alone decreased with increasing distance between the FA-branching carbon atom and the glycerol ester bond.

Similar results were obtained when OAHPA replaced PAHSA within TAG estolide substrates. Again, ATGL+CGI-58 cleaved the glycerol ester bond more efficiently than ATGL alone or HSL (Fig. 2*B*). Also, with OAHPA-containing TAG estolides, the hydrolytic activity of ATGL+CGI-58 decreased with the distance of the branching carbon atom to the glycerol ester bond and was lowest for TAG estolides containing the 9-OAHPA. Thus, the overall lipolytic activity of ATGL+CGI-58 for the cleavage of the FAHFA–glycerol ester bond in branched TAG estolides followed the "branching-point rule" 9-OAHPA < 7-OAHPA < 5-OAHPA. In contrast, the unbranched TAG estolide 66:1 with ω-hydroxy FA (16-OAHPA) did not follow this rule, since the 16-OAHPA release by ATGL+CGI-58 or ATGL alone was higher than the 9-OAHPA release (compare Fig. 2 *B* and *C*), indicating the branching-point rule does not apply to linear TAG estolides like TAG estolide with 16-OAHPA.

ATGL+CGI-58 Hydrolyzes Both *sn*-1,3 and *sn*-2 FAHFA–Glycerol Esters. To evaluate the regioselectivity of ATGL and HSL toward TAG estolides, we prepared positional isomers of the TAG estolide

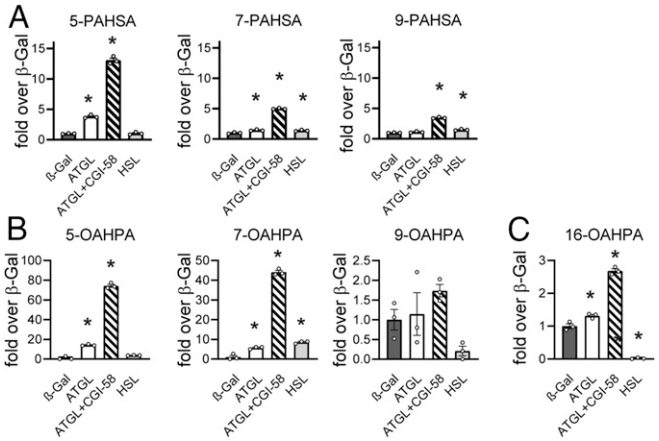

Fig. 2. The FAHFA–glycerol ester bond in TAG estolides is preferentially hydrolyzed by ATGL. (*A*) Release of PAHSAs from TAG estolide 66:0 with 5-, 7-, or 9-PAHSA bound at the *sn*-1/3 position. (*B*) Release of 5-, 7-, or 9-OAHPAs from TAG estolide 66:1 series. (*C*) Release of 16-OAHPA from the TAG estolide 66:1 with 16-OAHPA bound at the *sn*-1/3 position. Data are presented as means ± SEM ($n = 3$). Statistical differences were determined by one-way ANOVA with multiple comparison test (Tukey). *Significantly different at $P < 0.05$ from the β-Gal group. Additional statistics are presented in *SI Appendix*.

70:4 with 5-PAHSA esterified at a primary alcohol position (*sn*-1/3) or at the secondary alcohol position (*sn*-2) in the glycerol. While HSL remained a poor FAHFA–glycerol ester bond hydrolase, ATGL and ATGL+CGI-58 cleaved both *sn*-1,3 and *sn*-2 FAHFA–glycerol ester bonds, leading to the formation of free 5-PAHSA and the corresponding DAG 36:4 (Fig. 3*A*). In addition to the FAHFA–glycerol ester bond, ATGL+CGI-58 also cleaved the FA–glycerol ester bond, leading to the formation of linoleic acid (18:2) and the remaining DAG estolides (Fig. 3*B*). Notably, ATGL+CGI-58 as well as ATGL alone also led to the formation of MAG 18:2 (Fig. 3*A*) and the MAG estolide with 5-PAHSA (Fig. 3*B*), which may either result from DAG lipase or transacylase activities of ATGL (discussed below).

ATGL's Hydrolase and Transacylase Activities Generate TAG Double and Triple Monoestolides. Next, we assessed whether TAG estolide remodeling occurs via transesterification reactions. In addition to its hydrolytic activity, ATGL exhibits marked transacylase activity with MAGs or DAGs acting as acyl donors and DAGs as acyl acceptors, thus creating TAGs and glycerol or TAGs and MAGs, respectively (17, 19). Incubation of the TAG estolide 70:4 (5-PAHSA at the *sn*-1/3 position) with ATGL+CGI-58, but not ATGL alone or HSL, led to the formation of the TAG double monoestolides 84:0, 86:0, and 86:2 with FA 16:0, 18:0, and 18:2 as the third acyl chain as well as the TAG triple monoestolide 102:0 (Fig. 4*A*). Fig. 4*A* also includes the anticipated hydrolysis and transesterification reactions that led to these products. Fig. 4 *B*–*F* summarize a comprehensive analysis of selected reaction products of TAG estolide 70:4 incubation with ATGL+CGI-58. Transesterification and hydrolysis processes involved both the TAG estolide 70:4 substrate and acylglycerols that are present in the ATGL-overexpressing cell lysates, which markedly increased the compositional complexity of detected intermediates. This observation explains, for example, the appearance of monoestolides containing palmitic acid (Fig. 4 *B* and *C*) or myristic acid (Fig. 4*E*), which are not present in the TAG estolide substrate.

Taken together, ATGL+CGI-58 efficiently hydrolyzes the FAHFA–glycerol ester bond in TAG estolides depending on the FAHFA *sn* position and the branching carbon atom. Additionally, ATG+CGI-58 leads to major acylglycerol remodeling reactions that participate in the synthesis of TAG, DAG, and MAG estolides with FAHFAs in all *sn* positions as well as double and triple monoestolides.

Estolide Bond Hydrolysis: HSL Is the Major Estolide Bond Hydrolase. The striking drop of 16-OAHPA levels below control baseline in the HSL group (Fig. 2*C*) urged us to explore the hydrolysis of the estolide bond. Initially, we focused on the estolide bond hydrolysis in TAG estolides 66:1 with OAHPA branching at carbon atom 5, 7, or 9, and the unbranched 16-OAHPA. Estolide bond hydrolysis was monitored by the formation of oleic acid (FA 18:1). HSL-containing HEK293T lysates effectively hydrolyzed the estolide bond of all branched glycerol-bound FAHFAs with similar efficiency (Fig. 5 *A* and *B*). Extremely high hydrolytic activities of the enzyme were observed for the unbranched 16-OAHPA–containing TAG estolide. This profound activity enabled the detection of the second reaction product, TAG-containing 16-HPA [TAG 48:0(OH)] (Fig. 5*B*), which was undetectable when branched TAG estolides (Fig. 5*A*) were used as substrates. In comparison to HSL, ATGL alone or ATGL+CGI-58 did not hydrolyze the estolide bond in branched TAG estolides and exhibited a much weaker activity for the unbranched TAG estolide substrate containing 16-OAHPA (Fig. 5 *A* and *B*).

To investigate whether HSL also hydrolyzes nonesterified FAHFAs, we used the branched 5-, 7-, and 9-OAHPA as well as the unbranched 16-OAHPA as substrate in our lipase assays. HSL released oleic acid (FA 18:1) from all substrates. Highest enzyme activity was observed when the unbranched 16-OAHPA was used as substrate followed by 5-OAHPA, 7-OAHPA, and 9-OAHPA (Fig. 6*A*). Oleic acid release correlated well with the formation of the corresponding HFAs (Fig. 6*B*). In contrast to HSL, ATGL lacks or demonstrates only minor hydrolytic activity against OAHPA substrates.

The Loss of Functional ATGL or HSL Affects the TAG Estolide Metabolism in Mice. Finally, to assess whether the ATGL and HSL play a role in TAG estolide formation or hydrolysis also in vivo, TAG estolide and FAHFA concentrations were determined in white adipose tissue extracts from wild-type (WT), and ATGL and HSL knockout

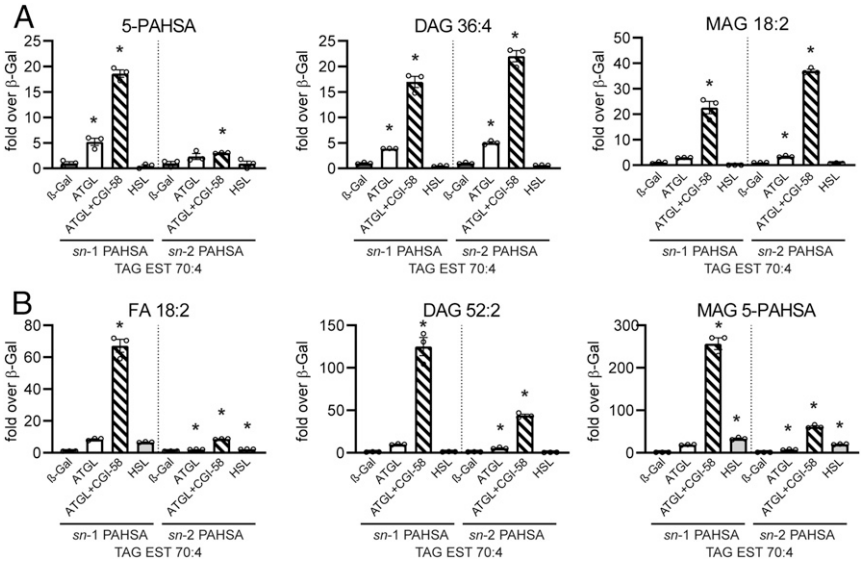

Fig. 3. Regioselectivity of ATGL-, ATGL+CGI-58–, and HSL-mediated glycerol ester bond hydrolysis. (*A* and *B*) Lipolytic products formed by the hydrolysis of TAG estolide (TAG EST) 70:4 with 5-PAHSA bound at *sn*-1/3 (marked *sn*-1 due to ATGL position specificity) or *sn*-2 position are shown. Data are presented as means ± SEM ($n = 3$). Statistical differences were determined by one-way ANOVA with multiple comparison test (Tukey). *Significantly different at $P < 0.05$ from the β-Gal group. Additional statistics are presented in *SI Appendix*. DAG 52:2 stands for DAG 5-PAHSA_18:2.

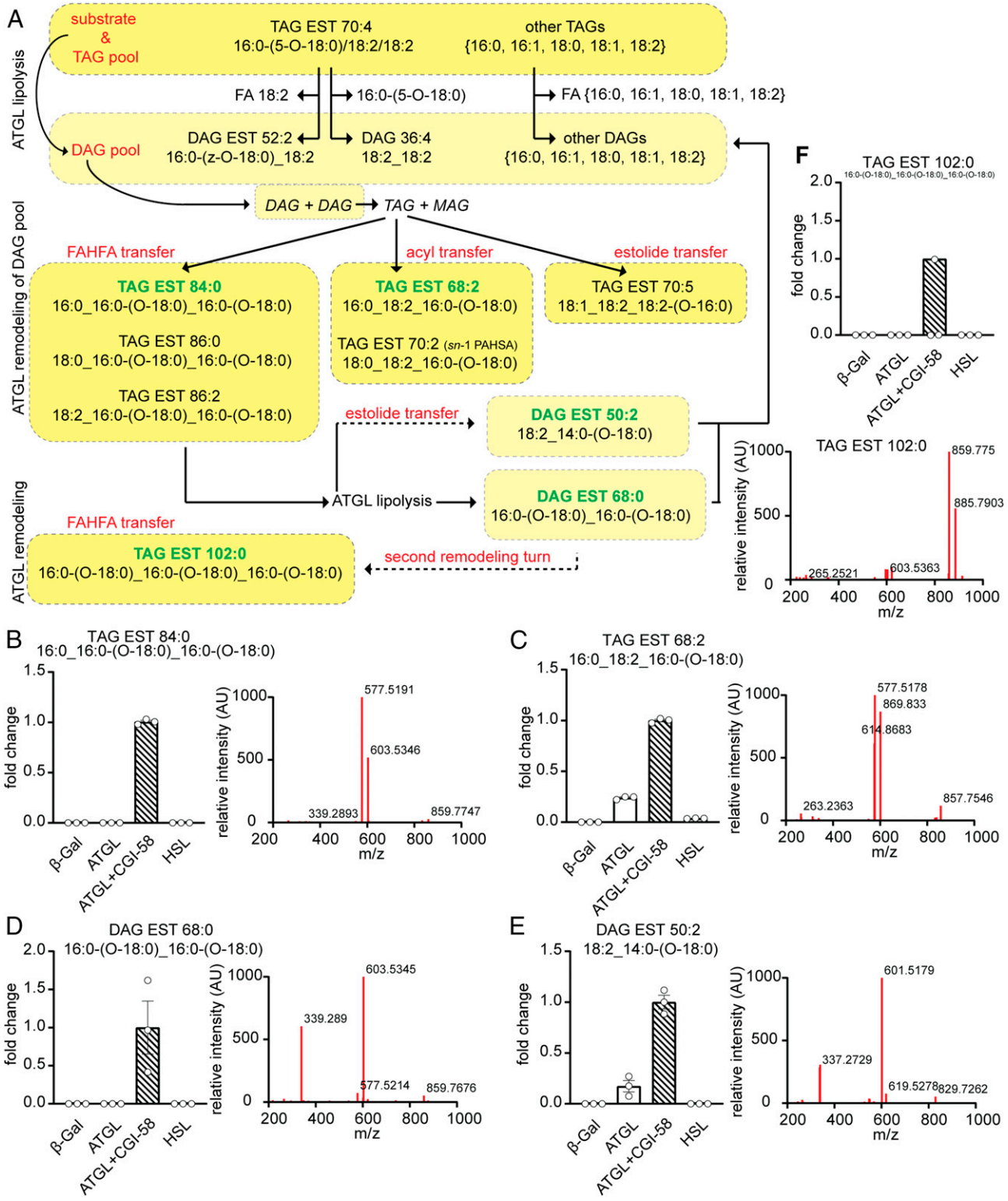

Fig. 4. TAG estolide remodeling yields alternative TAG estolide combinations. (*A*) Schematic representation of the main biochemical reactions running simultaneously or sequentially within the TAG estolide (TAG EST) 70:4 (5-PAHSA at *sn*-1/3) hydrolysis assay. The substrate as well as other substrates present in the cell lysate are metabolized by ATGL and other enzymes in the lysate. These pools of intermediates serve as both acyl donors and acceptors in reactions catalyzed by ATGL (acyltransferase, transacylase reaction). TAG estolides with one, two, or three PAHSAs and alternative estolides originating from FAHFA transfer or estolide remodeling were detected mainly in the samples where ATGL was coactivated by CGI-58. All structures with acyl chain composition were annotated based on MS/MS spectra. (*B*–*F*) Levels of selected estolides from *A* including MS/MS spectra. Data are presented as means ± SEM ($n = 3$). Fold change over ATGL+CGI-58 group.

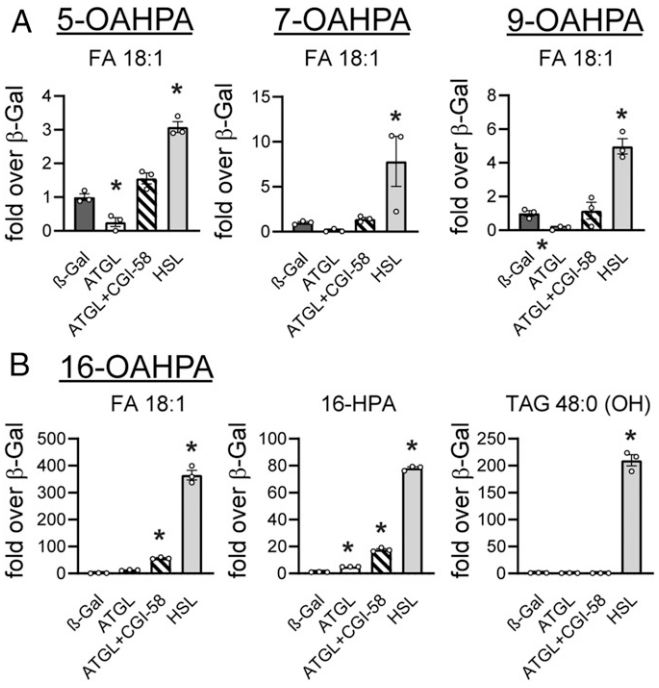

Fig. 5. The estolide bond in TAG estolides is preferentially hydrolyzed by HSL. Hydrolysis of TAG estolide 66:1 series with OAHPA bound at the *sn*-1/3 position and with OAHPA branching at the carbon atom 5, 7, 9 (*A*), and 16 (*B*), respectively. Data are presented as means ± SEM (n = 3). Statistical differences were determined by one-way ANOVA with multiple comparison test (Tukey). *Significantly different at $P < 0.05$ from the β-Gal group. Additional statistics are presented in *SI Appendix*. TAG 48:0(OH), monohydroxylated TAG intermediate; HPA, hydroxy palmitic acid. The 5-, 7-, and 9-HPA and the corresponding TAGs 48:0 (OH) were not found in *A* reactions.

(KO) mice. We previously reported that total TAG estolide levels decrease in ATGL-deficient adipose tissue (3). As shown in Fig. 7*A*, this decrease affects essentially all TAG estolide species in both the fed and the fasted state when compared to WT animals. Additionally, the variety of TAG estolides is reduced in ATGL-deficient adipose tissue, consistent with an essential role of ATGL-mediated transacylation reactions in the synthesis and remodeling of TAG estolides.

In contrast to the results in ATGL KO adipose tissue, essentially all species of TAG estolides increased in mice lacking adipose tissue HSL in both the fed and the fasted condition (Fig. 7*B*). Upon quantitation, total TAG estolide levels in HSL KO adipose tissue were approximately fourfold higher in the fed state and approximately eightfold higher in the fasted state when compared to WT animals (Fig. 7*C*), suggesting a crucial role of the enzyme in the degradation of TAG estolides. Furthermore, the concentrations of nonesterified FAHFAs were also increased in HSL KO adipose tissue (Fig. 7*D*). For example, the physiologically most relevant 5- and 9-PAHSA as well as 5- and 9-OAHPA increased 2- to 10-fold in adipose tissue of HSL KO mice in both the fasted and the fed condition.

Discussion

The current study addressed the question whether and how the principal metabolic lipases ATGL and HSL facilitate the hydrolysis of estolides and TAG estolides. In vitro enzyme activity assays revealed that both enzymes contribute to TAG estolide catabolism but differ in their substrate specificity. ATGL predominantly cleaves the ester bond between glycerol and FAHFAs but represents a relatively poor hydrolase for the estolide ester bond linking FAs to HFAs. ATGL additionally exhibits transacylase activity that is heavily involved in the remodeling of TAG estolides. In contrast, HSL is a much better estolide ester hydrolase (generating FA and HFA) than ATGL but a relatively weak enzyme to release FAHFAs from the glycerol backbone of TAG estolides. Moreover, HSL does not contribute to TAG estolide remodeling via catalysis of transacylase reactions. These findings strongly argue for distinct roles of the main enzymes for neutral lipolysis in estolide and TAG estolide metabolism.

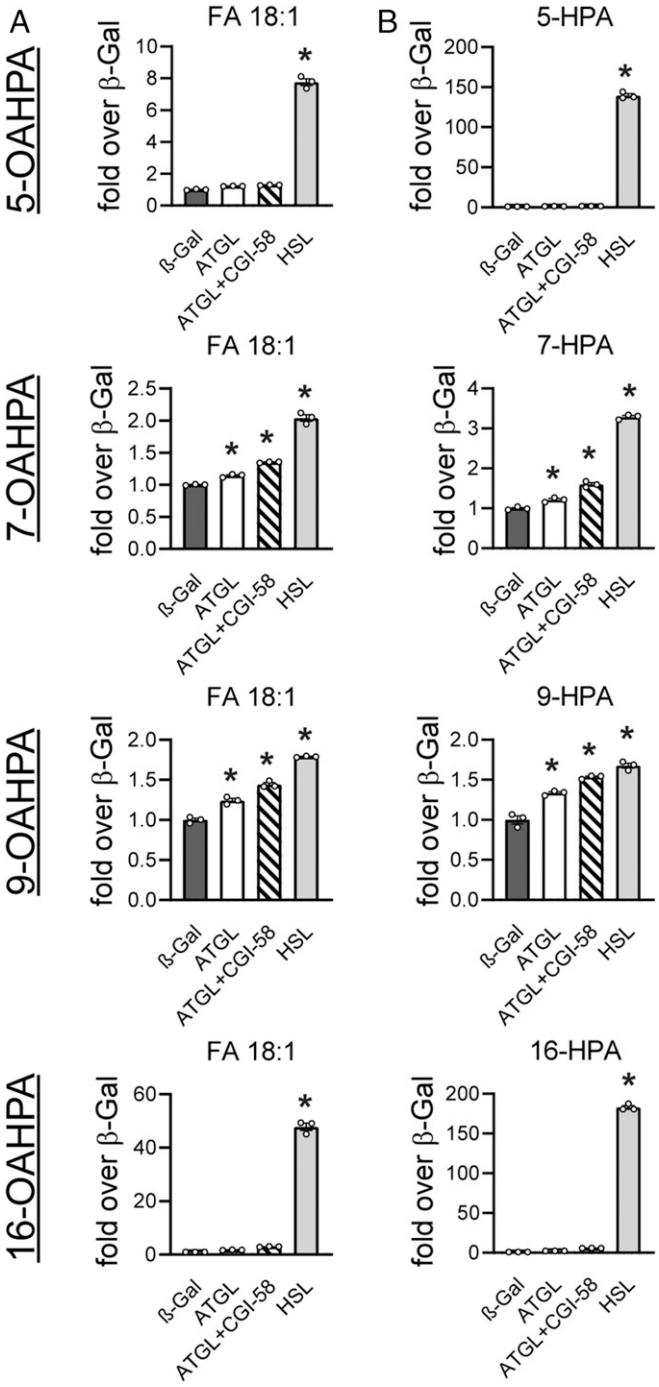

Fig. 6. Hydrolysis of free OAHPAs with branching at the carbon atom 5, 7, 9, or 16. Production of FA 18:1 (*A*) and the corresponding HPA (*B*). Data are presented as means ± SEM (n = 3). Statistical differences were determined by one-way ANOVA with multiple comparison test (Tukey). *Significantly different at $P < 0.05$ from the β-Gal group. Additional statistics are presented in *SI Appendix*.

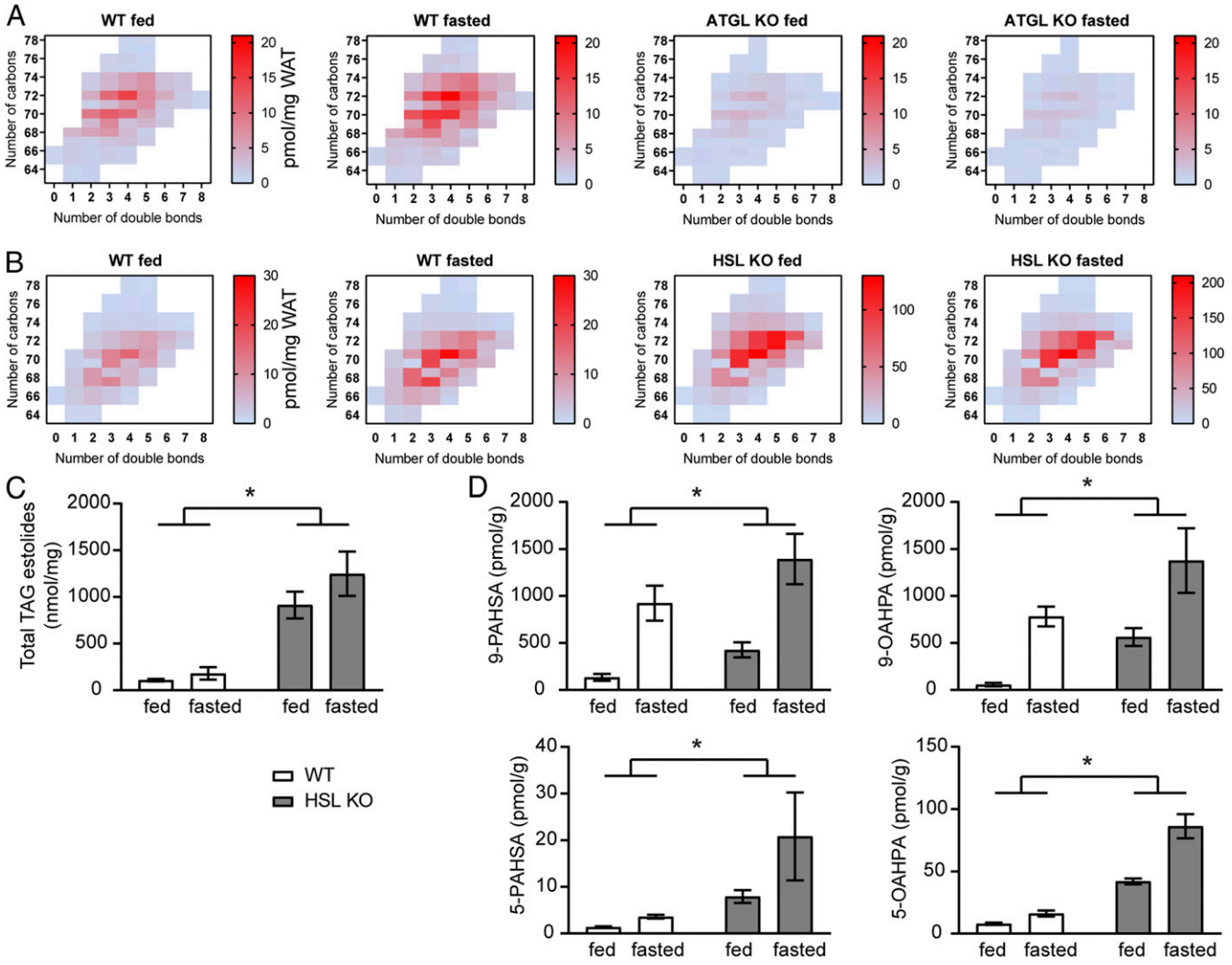

Fig. 7. Concentrations of TAG estolides and free FAHFAs in epididymal white adipose tissue of ATGL and HSL KO mice. Epididymal white adipose tissue from WT, ATGL KO, and HSL KO mice was collected in the ad libitum-fed and 14-h-fasted state. (*A* and *B*) TAG estolide species were quantified and data sorted according to the number of carbon atoms and the number of double bonds. The color scale represents the mean concentration ($n = 5$ to 7). When multiple isomers were detected, the square was divided into sections. (*C*) Concentrations of total TAG estolide and (*D*) various free FAHFAs in HSL KO white adipose tissue compared to WT control samples. Data are presented as means ± SEM ($n = 5$). Statistical differences were determined by two-way ANOVA with multiple comparison test (Tukey). *Significantly different at $P < 0.05$ for genotype. Additional statistics are presented in *SI Appendix*.

ATGL and HSL are highly expressed in white and brown adipose tissue, which are also primary sites of FAHFA and TAG estolide synthesis and metabolism. Nonadipose tissues including the heart, skeletal muscle, liver, pancreas, ovaries, or testes also express both enzymes at a lower level (18). Nevertheless, the severe pathology and increased lethality of ATGL deficiency in humans and mice highlights the functional importance of lipases in nonadipose tissues (35). Although both ATGL and HSL are potent TAG hydrolases, their substrate preferences differ. While ATGL preferentially hydrolyzes TAGs and requires FA chain lengths of eight carbon atoms and above with a modest preference for unsaturated over saturated FAs (26), HSL is much less substrate-specific, efficiently hydrolyzing TAGs, DAGs, MAGs, cholesteryl esters, retinyl ester, and short-chain ester substrates such as *p*-nitrophenylbutyrate (36). Therefore, it was not unexpected to find that ATGL and HSL hydrolyze various ester bonds within TAG estolides with different efficiency.

As observed for ATGL-mediated hydrolysis of regular TAGs, CGI-58 strongly enhanced enzyme activity also for TAG estolides. Our experimental setup did not permit a quantitative comparison of ATGL activities for ester hydrolysis of the TAG FAHFA-glycerol bond vs. TAG FA-glycerol bonds. However, from a rough estimation we can say that estolides are poorer substrates (1 to 10%) than ordinary FA esters. Concerning substrate specificity, ATGL favored branched TAG estolides with more compact structures, in which the branching carbon atom of FAHFAs is located closer to the glycerol backbone. This branching point-specific preference of ATGL may enable the preferential release of a subgroup of FAHFAs with specific biological functions. Unlike the majority of animal and bacterial lipases, ATGL+CGI-58 hydrolyzes ester bonds within TAGs at both the *sn*-1 and the *sn*-2 position (26, 37). This substrate preference was also observed when CGI-58–activated ATGL reacted with both positional isomers of TAG estolide 70:4 with 5-PAHSA bound to the *sn*-1/3 or the *sn*-2 position, resulting in the formation of free 5-PAHSA and the corresponding DAG. HSL also acted as a TAG estolide lipase generating FAHFAs and DAGs. However, compared to ATGL+CGI-58, the hydrolytic activity of HSL for the FAHFA–glycerol ester bond was considerably lower. This finding confirms previous studies using 3T3-L1 adipocytes and

ATGL as well as HSL inhibitors (15). ATGL and HSL are currently the only enzymes known that hydrolyze the FAHFA–glycerol ester bond on TAG estolides. Whether other established TAG hydrolases that are present in adipose tissue including carboxyl esterase-3 (CES3; also named triglyceride hydrolase-1) (38), PNPLA3 (also named adiponutrin) (39), or DDHD2 (40) also contribute to TAG estolide hydrolysis remains to be determined.

In addition to the well-established hydrolytic activity, both ATGL and HSL also exhibit transacylase activities, transferring acyl residues from donor acylglycerols to acceptor acylglycerols (17, 19). We previously demonstrated that although FAHFAs are released from TAG estolides during lipolysis, some FAHFAs and TAG estolides are being resynthesized at the same time (3). Our current data suggest that transacylation reactions catalyzed by CGI-58–activated ATGL are responsible for both processes. Apparently, ATGL reuses DAG estolides as acyl acceptors or donors to generate TAG estolides with an alternative acyl composition. This extensive remodeling process can result in the formation of double or triple estolides with two or three FAHFAs esterified to glycerol. However, the condensation of several FAHFAs on a single glycerol backbone is rare and only observed with PAHSA-containing substrates. Thus, we and others have only detected TAG monoestolides containing various FAHFAs in human and mouse white adipose tissue samples but failed to observe more complex di- and triestolide structures (3, 15, 16). TAG estolide analyses of ATGL-deficient white adipose tissue support the concept of a crucial role of ATGL in the synthesis and remodeling of FAHFAs and TAG estolides. Mice lacking ATGL have very low TAG estolide and nonesterified PAHSA levels in adipose tissue (3). ATGL-dependent PAHSA production may be physiologically relevant because under normal conditions free PAHSA concentrations rise in subcutaneous and perigonadal adipose tissue during fasting when ATGL expression is high in order to gear adipocytes for prospective glucose utilization (2, 3). In the absence of ATGL, low PAHSA concentrations may interfere with this normal fasting response. Taken together, the ATGL-mediated hydrolysis and transacylase reactions contribute to the formation and remodeling of FAHFAs and TAG estolides in vitro and in vivo, although details of these anabolic functions of ATGL remain to be elucidated.

Besides ATGL, other members of the PNPLA family have also been shown to catalyze transacylation reactions (41). PNPLA1 catalyzes the estolide bond formation between amide-linked ultra-long-chain HFAs in ω-hydroxyceramides and linoleic acid generating ω-*O*-acylceramides in keratinocytes. This reaction, utilizing TAG as acyldonor, is activated by CGI-58 and represents an essential step in the formation of the corneocyte lipid envelope to maintain permeability barrier function in the skin (42, 43). The second ATGL paralog, PNPLA3, also exhibits, in addition to its relatively weak TAG hydrolase activity, transacylase and acyltransferase activities (19, 44). Recent findings showed that PNPLA3 competes with ATGL for CGI-58 binding affecting TAG metabolism in adipocytes and hepatocytes (39, 45). In contrast to ATGL, *Pnpla3* gene expression is upregulated by insulin, which suggests a role in glycerolipid synthesis and remodeling rather than its degradation (46). While PNPLA1 expression is essentially restricted to keratinocytes, PNPLA3 is strongly expressed in adipose tissue and the liver. Whether PNPLA1 or 3 participate in FAHFA or TAG estolide synthesis and/or remodeling needs to be elucidated.

Our work identified HSL as a potent hydrolase of the estolide bond in FAHFAs and TAG estolides in vitro and in vivo. The absence of HSL resulted in a marked increase in total TAG estolide concentrations in white adipose tissue from fed and fasted mice. Free FAHFA concentrations also increased in HSL KO adipose tissue, arguing for a functional role of HSL as FAHFA hydrolase in branched FA metabolism also in vivo. Several other hydrolases including androgen-induced gene 1 (AIG1) protein, androgen-dependent TFPI regulating protein (ADTRP), and CES3 have already been identified as potential FAHFA hydrolases (47–49). Induced mutant mouse models proved that AIG1 and ADTRP are active estolide bond hydrolases in vivo (49). HSL adds to this list of hydrolases that affect tissue TAG estolide and FAHFA levels. The quantitative contribution of any of these lipases in different physiological situations is currently difficult to estimate and will depend on concomitant parameters such as tissue-specific expression levels, phosphorylation and activation state, and substrate preferences.

In conclusion, our results indicate that the predominant cellular neutral lipid hydrolases ATGL and HSL differently engage in the hydrolysis and remodeling of TAG estolides and FAHFAs. These distinct differences in hydrolase and transacylase activities, substrate specificity, and ester bond preference as well as a likely interaction with other known and possibly unknown enzymes create a complex enzymology in the formation of signaling FAHFAs that requires better characterization.

Methods

Nomenclature. The lipid nomenclature used throughout the paper is based on general literature recommendations and customized to describe the FAHFA-containing structures (2, 50). Briefly, the notation X:Y refers to an FA chain, where X is the total number of carbon atoms and Y is the number of double bonds.

FAHFAs belong to a family of estolides defined as mono- or oligomers of FAs. An estolide is characterized by the number of estolide linkages per molecule (estolide number, number of oligomers). Therefore, a FAHFA is a monoestolide (e.g., 9-PAHSA). Common (trivial) nomenclature of FAHFAs is used for the most-studied compounds like 9-PAHSA, where 9 defines the ester position relative to carboxylic acid and PA and HSA stand for palmitic acid and hydroxy stearic acid, respectively. Alternatively, to avoid abbreviations for each FA, generalized nomenclature X1:Y1-(z-O-X2:Y2) [e.g., 16:0-(9-O-18:0) for 9-PAHSA] is used for schematic representations.

TAG estolide nomenclature follows the general recommendations and an FAHFA is treated as an acyl group (51). Where only one FAHFA is bound to the glycerol backbone, it is a TAG monoestolide. Where two or three FAHFAs are bound to glycerol, it is a double or triple TAG monoestolide, respectively. As only monoestolides (FAHFAs) were found in mammals, the "mono" prefix is often omitted. The position of the FAHFA or FA acyl chains on the glycerol backbone is reported in the order *sn*-1, *sn*-2, *sn*-3, from left to right. As an example, when 9-PAHSA is esterified at the *sn*-1/3 position of the racemic 1,2-dipalmitoyl glycerol, the structure is written as 16:0-(9-O-18:0)/16:0/16:0, while an unknown position of the 9-PAHSA in the glycerol backbone is written 16:0-(9-O-18:0)_16:0_16:0.

Reagents. All chemical reagents were from Sigma-Aldrich unless stated otherwise. FAHFA standards were from Cayman Europe or synthesized previously (34).

TAG Estolide Library. The TAG estolides were synthesized at the Institute of Biomolecules Max Mousseron (Montpellier) and the Institute of Organic Chemistry and Biochemistry. The procedure for the Steglich esterification reactions is exemplified with the synthesis of TAG estolide 66:0 (*SI Appendix*). The synthesis of TAG estolide 70:4 is outlined in Fig. 1*A*.

cDNA Cloning of Recombinant Proteins and Expression and Purification of SMT-Tagged CGI-58. Mammalian expression vector pcDNA4/HisMax constructs containing the entire open reading frame of murine ATGL, murine HSL, or LacZ (β-Gal) were generated as described in Lass et al. (22). Small ubiquitin-like modifier (SMT)-tagged CGI-58 was expressed and purified as described in Gruber et al. (21).

Expression of Recombinant Proteins. HEK293T cells (ATCC CRL-3216) were cultivated in Dulbecco's modified Eagle's medium (Thermo Fisher Scientific) supplemented with 10% fetal bovine serum on cell culture dishes precoated with 0.1% gelatin in a standard humidified 7% CO_2 atmosphere at 37 °C; 1×10^6 cells were transfected with 2.5 μg plasmid DNA using Metafectene (Biontex GmbH) according to the manufacturer's instructions. The expression of Xpress-tagged proteins was detected using Western blotting analysis as described previously (42).

Preparation of Cell Homogenates. HEK293T cells overexpressing β-Gal, ATGL, or HSL were harvested 24 h after transfection and disrupted in buffer A (0.25 mol/L sucrose, 1 mmol/L ethylenediaminetetraacetic acid, 1 mmol/L dithiothreitol, pH 7.0, supplemented with 1 μg/mL pepstatin, 2 μg/mL antipain, and 20 μg/mL leupeptin) by sonication on ice. Thereafter, the cell lysates were centrifuged at 1,000 × *g* and 4 °C for 10 min to pellet the nuclei and unbroken cells. The protein concentration of the supernatants was determined using the Bradford reagent (Bio-Rad) and bovine serum albumin as a standard.

TAG Estolide Hydrolysis Assay. For the determination of TAG estolide hydrolase activity of HSL and ATGL in the presence or absence of CGI-58, 50 μg of protein from the respective cell homogenates was mixed with 200 ng of purified SMT-tagged CGI-58 or SMT empty vector control in a total volume of 100 μL of buffer A and then incubated with 100 μL of substrate in a water bath at 37 °C for 60 min. The reaction was terminated by adding 1 mL of methyl *tert*-butyl ether/methanol/acetic acid (75/25/1, vol/vol/vol). After centrifugation (7,500 × *g*, 5 min, room temperature), the organic phase was collected, dried under a stream of nitrogen, and finally resuspended in a dichloromethane/methanol/isopropanol (1/2/4, vol/vol/vol) mixture. Reaction products were analyzed using lipidomics platforms. As a control, incubations were performed under identical conditions using homogenates from cells expressing β-Gal that does not exhibit hydrolytic activities. To identify lipid products formed by the reaction of background lipids present in cell homogenates, control reactions were performed under identical conditions without the TAG estolide substrate. The assay substrate contained 250 μmol/L TAG estolide emulsified with 35 μmol/L phosphatidylcholine/phosphatidylinositol (PC/PI, 3:1) in 100 mmol/L potassium phosphate buffer, pH 7.0, by sonication on ice. To prevent product inhibition, bovine serum albumin was added to the reaction at a final concentration of 1%. Assays with free OAHPAs, triolein, or diolein as substrate were processed identically.

Animal Tissues. White adipose tissue was prepared from ad libitum-fed and 12- to 14-h-fasted, 12- to 14-wk-old female global HSL KO (53) and ATGL KO (52) mice as well as corresponding WT controls. Mice were housed under standard conditions (25 °C, 14/10-h light/dark cycle) with ad libitum access to chow diet (11 kJ % fat, V1126; Ssniff Spezialdiäten GmbH) in a specific pathogen-free environment. All animal studies were approved by the Ethics committee of the University of Graz and the Austrian Federal Ministry of Science, Research and Economy.

Lipidomics. The LC-MS system consisted of a Vanquish UHPLC System (Thermo Fisher Scientific) coupled to a Q Exactive Plus mass spectrometer (Thermo Fisher Scientific). For the acylglycerol estolide platform, the MS1 mass range of *m/z* 400 to 2,000 was used. Data were acquired in positive electrospray ionization (ESI) mode with a spray voltage of 3.6 kV and normalized collision energy of 20%. General lipidomic profiling in both positive and negative mode was performed as described before (3). TAG estolides are detectable in positive ion mode, similar to TAGs, as ammoniated adducts, sodium adducts, or ethylamine adducts $[M+CH_3CH_2NH_2+H]^+$ if acetonitrile is used as solvent.

Using this methodology, the TAG estolide mixture could be separated according to the number of carbon atoms and double bonds, and individual superfamilies (e.g., 70:4) could be quantified. For LC-ESI(+)-MS analysis, the mobile phase consisted of (A) 60:40 (vol/vol) acetonitrile:water with ammonium formate (10 mmol/L) and formic acid (0.1%) and (B) 90:10:0.1 (vol/vol/vol) isopropanol:acetonitrile:water with ammonium formate (10 mmol/L) and formic acid (0.1%); the following prolonged gradient was used: 0 min 0% (B); 0 to 12 min from 0 to 95% (B); 12 to 18 min from 95 to 99% (B); 18 to 25 min at 99% (B); 25 to 27 min from 99 to 0% (B); and 27 to 35 min 0% (B) (3). TAG estolide quantification was performed using deuterated TAG internal standards (TAG 51:1-$^2H_5$, TAG 60:1-$^2H_5$) and confirmed by the method of standard addition of pure TAG estolide 70:4 (3). The FA composition of the TAG estolide (or the main contributor) within the superfamily can be deduced from the MS/MS spectra, thus allowing the assessment of TAG estolide acyl composition as before (3). See the extracted ion chromatograms in *SI Appendix*, pages S60–S61.

Bioinformatics and Statistical Analyses. LC-MS and LC-MS/MS data were processed with the software MS-DIAL v. 4.0 (54). Metabolites were annotated using an in-house retention time–*m/z* library, and an in silico library of theoretical acylglycerol estolides was calculated using Python scripts. GraphPad Prism 8.0.2 was used to compare groups (ANOVA, Tukey's multiple comparisons test).

Data Availability. All study data are included in the paper and *SI Appendix*.

ACKNOWLEDGMENTS. This work was supported by grants from the Czech Science Foundation (20-00317S) and the Czech Academy of Sciences (LQ200111901; RVO Grant 61388963), projects P 32225-B (to F.P.W.R.) and F7302 SFB LIPID HYDROLYSIS (to R.Z.) funded by the Austrian Funds zur Förderung der Wissenschaftlichen Forschung, the Fondation Leducq Transatlantic Network grant 12CVD04 (R.Z.), the Louis-Jeantet Prize for Medicine 2015 (R.Z.), and the European Research Council (ERC) under the European Union's Seventh Framework Programme (FP/2007-2013)/ERC Grant Agreement 340896 (R.Z.). We thank Dr. Martin Dracinsky for measuring samples.

1. J. Lee *et al.*, Branched fatty acid esters of hydroxy fatty acids (FAHFAs) protect against colitis by regulating gut innate and adaptive immune responses. *J. Biol. Chem.* **291**, 22207–22217 (2016).
2. M. M. Yore *et al.*, Discovery of a class of endogenous mammalian lipids with antidiabetic and anti-inflammatory effects. *Cell* **159**, 318–332 (2014).
3. V. Paluchova *et al.*, Lipokine 5-PAHSA is regulated by adipose triglyceride lipase and primes adipocytes for de novo lipogenesis in mice. *Diabetes* **69**, 300–312 (2020).
4. A. Hammarstedt *et al.*, Adipose tissue dysfunction is associated with low levels of the novel Palmitic Acid Hydroxystearic Acids. *Sci. Rep.* **8**, 15757 (2018).
5. B. Bandak, L. Yi, M. G. Roper, Microfluidic-enabled quantitative measurements of insulin release dynamics from single islets of Langerhans in response to 5-palmitic acid hydroxy stearic acid. *Lab Chip* **18**, 2873–2882 (2018).
6. I. Syed *et al.*, PAHSAs attenuate immune responses and promote β cell survival in autoimmune diabetic mice. *J. Clin. Invest.* **129**, 3717–3731 (2019).
7. O. Kuda *et al.*, Docosahexaenoic acid-derived fatty acid esters of hydroxy fatty acids (FAHFAs) with anti-inflammatory properties. *Diabetes* **65**, 2580–2590 (2016).
8. I. Syed *et al.*, Palmitic acid hydroxystearic acids activate GPR40, which is involved in their beneficial effects on glucose homeostasis. *Cell Metab.* **27**, 419–427.e4 (2018).
9. K. Brejchova *et al.*, Understanding FAHFAs: From structure to metabolic regulation. *Prog. Lipid Res.* **79**, 101053 (2020).
10. Y. Z. Chen *et al.*, Fatty acid estolides: A review. *J. Am. Oil Chem. Soc.* **97**, 231–241 (2020).
11. O. Kuda *et al.*, Nrf2-Mediated antioxidant defense and peroxiredoxin 6 are linked to biosynthesis of palmitic acid ester of 9-hydroxystearic acid. *Diabetes* **67**, 1190–1199 (2018).
12. M. Brezinova *et al.*, Levels of palmitic acid ester of hydroxystearic acid (PAHSA) are reduced in the breast milk of obese mothers. *Biochim. Biophys. Acta Mol. Cell Biol. Lipids* **1863**, 126–131 (2018).
13. J. T. Lin, A. Arcinas, L. R. Harden, C. K. Fagerquist, Identification of (12-ricinoleoylricinoleoyl)diricinoleoylglycerol, an acylglycerol containing four acyl chains, in castor (Ricinus communis L.) oil by LC-ESI-MS. *J. Agric. Food Chem.* **54**, 3498–3504 (2006).
14. H. X. Zhang, D. J. H. Olson, D. Van, R. W. Purves, M. A. Smith, Rapid identification of triacylglycerol-estolides in plant and fungal oils. *Ind. Crops Prod.* **37**, 186–194 (2012).
15. D. Tan *et al.*, Discovery of FAHFA-containing triacylglycerols and their metabolic regulation. *J. Am. Chem. Soc.* **141**, 8798–8806 (2019).
16. M. Brezinova *et al.*, Exercise training induces insulin-sensitizing PAHSAs in adipose tissue of elderly women. *Biochim. Biophys. Acta Mol. Cell Biol. Lipids* **1865**, 158576 (2020).
17. C. M. Jenkins *et al.*, Identification, cloning, expression, and purification of three novel human calcium-independent phospholipase A2 family members possessing triacylglycerol lipase and acylglycerol transacylase activities. *J. Biol. Chem.* **279**, 48968–48975 (2004).
18. R. Zimmermann *et al.*, Fat mobilization in adipose tissue is promoted by adipose triglyceride lipase. *Science* **306**, 1383–1386 (2004).
19. X. Zhang *et al.*, An epistatic interaction between *Pnpla2* and *lipe* reveals new pathways of adipose tissue lipolysis. *Cells* **8**, 395 (2019).
20. A. C. Lake *et al.*, Expression, regulation, and triglyceride hydrolase activity of Adiponutrin family members. *J. Lipid Res.* **46**, 2477–2487 (2005).
21. A. Gruber *et al.*, The N-terminal region of comparative gene identification-58 (CGI-58) is important for lipid droplet binding and activation of adipose triglyceride lipase. *J. Biol. Chem.* **285**, 12289–12298 (2010).
22. A. Lass *et al.*, Adipose triglyceride lipase-mediated lipolysis of cellular fat stores is activated by CGI-58 and defective in Chanarin-Dorfman syndrome. *Cell Metab.* **3**, 309–319 (2006).
23. C. Lefèvre *et al.*, Mutations in CGI-58, the gene encoding a new protein of the esterase/lipase/thioesterase subfamily, in Chanarin-Dorfman syndrome. *Am. J. Hum. Genet.* **69**, 1002–1012 (2001).
24. Z. H. Jebessa *et al.*, The lipid droplet-associated protein ABHD5 protects the heart through proteolysis of HDAC4. *Nat. Metab.* **1**, 1157–1167 (2019).
25. G. Montero-Moran *et al.*, CGI-58/ABHD5 is a coenzyme A-dependent lysophosphatidic acid acyltransferase. *J. Lipid Res.* **51**, 709–719 (2010).
26. T. O. Eichmann *et al.*, Studies on the substrate and stereo/regioselectivity of adipose triglyceride lipase, hormone-sensitive lipase, and diacylglycerol-O-acyltransferases. *J. Biol. Chem.* **287**, 41446–41457 (2012).
27. G. Fredrikson, H. Tornqvist, P. Belfrage, Hormone-sensitive lipase and monoacylglycerol lipase are both required for complete degradation of adipocyte triacylglycerol. *Biochim. Biophys. Acta* **876**, 288–293 (1986).

BIOCHEMISTRY

28. M. Sekiya *et al*., Hormone-sensitive lipase is involved in hepatic cholesteryl ester hydrolysis. *J. Lipid Res.* **49**, 1829–1838 (2008).
29. J. A. Rodriguez *et al*., In vitro stereoselective hydrolysis of diacylglycerols by hormone-sensitive lipase. *Biochim. Biophys. Acta* **1801**, 77–83 (2010).
30. S. Wei *et al*., Retinyl ester hydrolysis and retinol efflux from BFC-1beta adipocytes. *J. Biol. Chem.* **272**, 14159–14165 (1997).
31. J. G. Granneman *et al*., Analysis of lipolytic protein trafficking and interactions in adipocytes. *J. Biol. Chem.* **282**, 5726–5735 (2007).
32. C. Krintel, M. Mörgelin, D. T. Logan, C. Holm, Phosphorylation of hormone-sensitive lipase by protein kinase A in vitro promotes an increase in its hydrophobic surface area. *FEBS J.* **276**, 4752–4762 (2009).
33. C. Krintel *et al*., Ser649 and Ser650 are the major determinants of protein kinase A-mediated activation of human hormone-sensitive lipase against lipid substrates. *PLoS One* **3**, e3756 (2008).
34. L. Balas *et al*., Regiocontrolled syntheses of FAHFAs and LC-MS/MS differentiation of regioisomers. *Org. Biomol. Chem.* **14**, 9012–9020 (2016).
35. M. Schweiger, A. Lass, R. Zimmermann, T. O. Eichmann, R. Zechner, Neutral lipid storage disease: Genetic disorders caused by mutations in adipose triglyceride lipase/PNPLA2 or CGI-58/ABHD5. *Am. J. Physiol. Endocrinol. Metab.* **297**, E289–E296 (2009).
36. T. Tsujita, H. Ninomiya, H. Okuda, p-nitrophenyl butyrate hydrolyzing activity of hormone-sensitive lipase from bovine adipose tissue. *J. Lipid Res.* **30**, 997–1004 (1989).
37. E. Rogalska, C. Cudrey, F. Ferrato, R. Verger, Stereoselective hydrolysis of triglycerides by animal and microbial lipases. *Chirality* **5**, 24–30 (1993).
38. K. G. Soni *et al*., Carboxylesterase 3 (EC 3.1.1.1) is a major adipocyte lipase. *J. Biol. Chem.* **279**, 40683–40689 (2004).
39. A. Yang, E. P. Mottillo, L. Mladenovic-Lucas, L. Zhou, J. G. Granneman, Dynamic interactions of ABHD5 with PNPLA3 regulate triacylglycerol metabolism in brown adipocytes. *Nat. Metab.* **1**, 560–569 (2019).
40. M. Araki *et al*., Enzymatic characterization of recombinant rat DDHD2: A soluble diacylglycerol lipase. *J. Biochem.* **160**, 269–279 (2016).
41. P. C. Kienesberger, M. Oberer, A. Lass, R. Zechner, Mammalian patatin domain containing proteins: A family with diverse lipolytic activities involved in multiple biological functions. *J. Lipid Res.* **50** (suppl.), S63–S68 (2009).
42. B. Kien *et al*., ABHD5 stimulates PNPLA1-mediated ω-*O*-acylceramide biosynthesis essential for a functional skin permeability barrier. *J. Lipid Res.* **59**, 2360–2367 (2018).
43. Y. Ohno, A. Nara, S. Nakamichi, A. Kihara, Molecular mechanism of the ichthyosis pathology of Chanarin-Dorfman syndrome: Stimulation of PNPLA1-catalyzed ω-O-acylceramide production by ABHD5. *J. Dermatol. Sci.* **92**, 245–253 (2018).
44. M. Kumari *et al*., Adiponutrin functions as a nutritionally regulated lysophosphatidic acid acyltransferase. *Cell Metab.* **15**, 691–702 (2012).
45. Y. Wang, N. Kory, S. BasuRay, J. C. Cohen, H. H. Hobbs, PNPLA3, CGI-58, and inhibition of hepatic triglyceride hydrolysis in mice. *Hepatology* **69**, 2427–2441 (2019).
46. E. E. Kershaw *et al*., Adipose triglyceride lipase: Function, regulation by insulin, and comparison with adiponutrin. *Diabetes* **55**, 148–157 (2006).
47. M. J. Kolar *et al*., Branched fatty acid esters of hydroxy fatty acids are preferred substrates of the MODY8 protein carboxyl ester lipase. *Biochemistry* **55**, 4636–4641 (2016).
48. W. H. Parsons *et al*., AIG1 and ADTRP are atypical integral membrane hydrolases that degrade bioactive FAHFAs. *Nat. Chem. Biol.* **12**, 367–372 (2016).
49. M. Erikci Ertunc *et al*., AIG1 and ADTRP are endogenous hydrolases of fatty acid esters of hydroxy fatty acids (FAHFAs) in mice. *J. Biol. Chem.* **295**, 5891–5905 (2020).
50. Y. Ma *et al*., An in silico MS/MS library for automatic annotation of novel FAHFA lipids. *J. Cheminform.* **7**, 53 (2015).
51. R. A. Moreau *et al*., The identification of mono-, di-, tri-, and tetragalactosyldiacylglycerols and their natural estolides in oat kernels. *Lipids* **43**, 533–548 (2008).
52. G. Haemmerle *et al*., Defective lipolysis and altered energy metabolism in mice lacking adipose triglyceride lipase. *Science* **312**, 734–737 (2006).
53. G. Haemmerle *et al*., Hormone-sensitive lipase deficiency in mice causes diglyceride accumulation in adipose tissue, muscle, and testis. *J. Biol. Chem.* **277**, 4806–4815 (2002).
54. H. Tsugawa *et al*., MS-DIAL: Data-independent MS/MS deconvolution for comprehensive metabolome analysis. *Nat. Methods* **12**, 523–526 (2015).